Structural Changes in Phase Transitions of Nylon Model Compounds. 1. Transition Behavior of Model Compounds of R-NHCO-R′ Type

Yayoi Yoshioka[†,‡] and Kohji Tashiro*[,†]

Department of Macromolecular Science, Graduate School of Science, Osaka University, Toyonaka, Osaka 560-0043, Japan, and Technology Research Institute of Osaka Prefecture, Izumi, Osaka 594-1157, Japan

Received: November 12, 2002; In Final Form: July 15, 2003

To clarify the essential features of Brill transition of aliphatic nylons, structural changes have been investigated by X-ray diffraction and infrared spectroscopic methods for the compounds $CH_3(CH_2)_{10}NHCO(CH_2)_9CH_3$ (designated as **N11**) and $CH_3(CH_2)_9NHCO(CH_2)_8CH_3$ (**N10**) which were assumed to be the simplest models of nylons 11/11 and 10/10, respectively. Depending on the preparation conditions, **N11** crystallized to the α and γ forms and **N10** to the α form at room temperature. Infrared and X-ray diffraction data clarified that the α form took essentially the same chain packing structure as that of the α form of parent nylons, in which the all-trans methylene segments were packed in a triclinic subcell and the amide groups were connected by intermolecular hydrogen bonds to form a sheet structure and these sheets were stacked by a weak van der Waals force. In the DSC thermograms, the α form of **N10** and **N11** showed two main endothermic peaks in the Brill transition (ca. 50 °C) and melting regions. The temperature region was divided into three (I, II, and III). In region I below 50 °C, the crystal was of the α type. In region III (above 58 °C for **N10** and above 65 °C for **N11**), the crystal transferred to the high-temperature γ form (γ_h), in which the molecular chains had disordered conformation, as speculated from the change in methylene progression bands and the broad amide bands, and these chains were packed in a pseudohexagonal mode. During the transition from region I to III, another phase was observed to appear discontinuously in region II. This intermediate phase showed the infrared spectra composed of the characteristic patterns of the α and γ_h forms but the X-ray diffraction pattern was quite unique and different from those of the latter two forms, indicating that the molecules with a hybrid conformation between the α and γ_h forms were packed in a unique crystal lattice. In case of the γ form of **N11** compound, the molecular chains took the conformation built by skewed amide groups and partially disordered trans methylene segments even at room temperature. The crystal transferred apparently continuously to the γ_h form above 70 °C.

Introduction

Thermally induced crystal structural changes of aliphatic polyamides or nylons are known as the Brill transition.[1] For example, nylon 6/6 shows the Brill transition at ca. 210 °C, where the α phase of triclinic structure transforms to the pseudo-hexagonal structure. Many papers had been published to clarify the structural changes in this transition, but the details have not yet been revealed.[1−19] As one of the most useful methods to solve these problems we may utilize the various kinds of low-molecular-weight model compounds having similar chemical structures with nylons. In a lucky case we might be able to prepare the single crystals, which would give us precise information about the chain conformation as well as the chain packing mode. At the same time, these model compounds might exhibit clear and sharp phase transitions. The information on structural changes occurring in these transitions is useful and basically important for understanding the essential features of the Brill transition of the parent nylons. However, there had been published only a limited number of reports concerning the structure and phase transition of these model compounds.[12,20−24]

Recently we prepared a series of model compounds of nylon *m*/*n* with the formulas R-NHCO-R′, R-NHCO-R″-CONH-R′, or R-CONH-R″-NHCO-R′ where R and R′ were $-(CH_2)_pCH_3$ groups and R″ was the $-(CH_2)_q-$ sequence, and we investigated the phase transition behavior through the measurement of the temperature dependence of X-ray diffraction and infrared spectra. In the present study, we will report the experimental data collected for the model compounds with the simplest chemical formula R-NHCO-R′ with R = $(CH_2)_9CH_3$ and R′ = $(CH_2)_8CH_3$ or R = $(CH_2)_{10}CH_3$ and R′ = $(CH_2)_9CH_3$. The former is named here **N10** and the latter **N11**, which may be assumed as the simplest model compounds of nylon 10/10 and nylon 11/11, respectively. Of course, the compounds with larger number of repeating units such as R-NHCO-R″-CONH-R′ etc. should be more ideal to study the essential behavior of the parent polymers. The experimental data collected for these longer compounds will be reported in a separate paper. However, it must be emphasized here that even for such simplest compounds as **N10** and **N11**, we have not yet obtained any detailed information on the structure and phase transition behavior on investigating the literature.

Nylons are known to crystallize into several types of crystal modifications depending on the crystallization conditions. The most representative modifications are α and γ forms.[25−29] In the α crystal form the all-trans (T) planar-zigzag chains are packed together with the intermolecular hydrogen bonds be-

* To whom correspondence should be addressed. E-mail: ktashiro@chem.sci.osaka-u.ac.jp.
† Osaka University.
‡ Technology Research Institute of Osaka Prefecture.

10.1021/jp0224160 CCC: $25.00
Published on Web 10/14/2003

tween the neighboring amide groups to form a sheet structure. These sheets are stacked by weak van der Waals forces. The molecular chains in the γ form take the slightly contracted conformation with the skew (S) and minus skew ($\bar{S}$) bonds

$$\text{-CH}_2\text{-NH-CO-CH}_2\text{-} \qquad \text{-CH}_2\text{-NH-CO-CH}_2\text{-}$$

$$\alpha\text{-form} \quad T\ T\ T \qquad \gamma\text{-form} \quad S\ T\ \bar{S}$$

around methylene−amide linkages and are packed in the unit cell through the intermolecular hydrogen bonds and weaker van der Waals force. Inner parts of the methylene sequences are in the trans-zigzag form. We have found **N11** crystallized into both the α and γ forms at room temperature, while **N10** crystallized only in the α form. In the present paper the temperature dependences of X-ray diffraction and infrared spectra are measured and the transition behaviors are compared in detail between the α and γ forms of **N11** and **N10**. As mentioned above, the information obtained for the simplest **N10** and **N11** compounds is expected to be helpful for the detailed study of longer model compounds and parent nylon samples.

Experimental Section

Samples. Model compounds $CH_3(CH_2)_{10}NHCO(CH_2)_9CH_3$ (**N11**) and $CH_3(CH_2)_9NHCO(CH_2)_8CH_3$ (**N10**) were synthesized by a condensation reaction of the corresponding *N*-alkyl chloride (R′-COCl) with *n*-alkylamine (R-NH_2) in the toluene solution. After the products were purified 3 times by reprecipitation from the ethanol solution into water, an elementary analysis was made: for **N11**, C 77.71% (prediction 77.81%), H 13.45% (13.36%), and N 4.13% (4.12%) and for N10, C 76.70% (prediction 77.10%), H 13.17% (13.26%), and N 4.43% (4.50%). The small crystals were obtained from the methanol or ethanol solutions at room temperature. The crystal modification was identified by the infrared spectra. **N10** gave only the α form. **N11** gave mostly the γ form but occasionally it crystallized into the α form. Although the details are not known yet, crystallization in lower temperature atmosphere tended to give the α form preferentially. These crystalline forms were named **N11**-α, **N11**-γ, and **N10**-α, respectively.

Measurements. DSC thermograms were measured in the heating process by using a differential scanning calorimeter SEIKO DSC220CU under nitrogen gas atmosphere at the rate of 4 deg/min. Temperature dependence of infrared spectra was measured for a KBr disk using a Digilab (Biorad) FTS-60A/896 Fourier transform infrared spectrometer at the resolving power of 1 cm^{-1}. The mechanically ground powder samples were used for the X-ray diffraction measurements. The temperature dependence of X-ray diffraction profiles was measured by using a Rigaku RINT-Ultima$^+$ X-ray diffractometer with a graphite-monochromatized Cu Kα line at a scanning rate of 1 deg/min.

Results and Discussion

DSC Thermograms. Figure 1 a, b, and c shows the DSC thermograms measured for **N10**-α, **N11**-α, and **N11**-γ in the heating process from 20 to 90 °C, respectively. In the case of the α form, both **N11** and **N10** showed a small endothermic peak around 50 °C in addition to a larger endothermic peak around 78 °C (**N11**-α) or 70 °C (**N10**-α), the latter peak being due to the melting phenomenon. It was very difficult to detect a peak in the temperature region between these two peaks but a clear structural change was found to occur: the X-ray diffraction pattern in this temperature region was different from

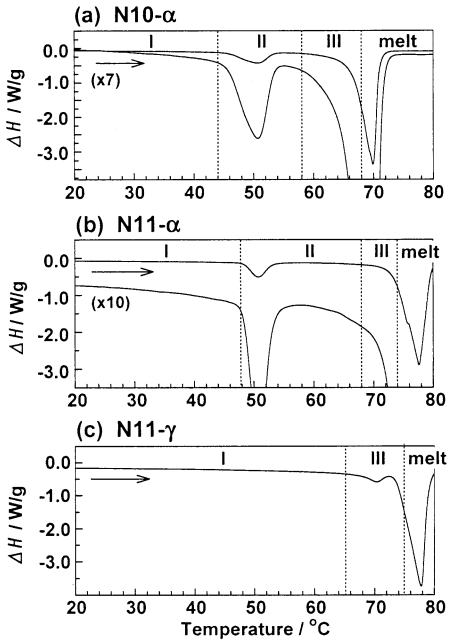

Figure 1. DSC thermograms in the heating process: (a) **N10**-α, (b) **N11**-α, and (c) **N11**-γ.

those observed in the other temperature regions as will be mentioned in a later section. Therefore, the DSC thermograms of **N10**-α and **N1**-α were divided into three temperature regions I, II, and III as shown in Figure 1. The **N11**-γ form showed a small peak around 70 °C in addition to the melting peak. The temperature regions were divided into two, I and III, for reasons mentioned later. The high-temperature phase was named III, not II, because of the similarity of structure with that found in the region III of the **N11**-α form. The enthalpy changes of the main two endothermic peaks were evaluated for these three samples: 23.0 and 161.3 J/g for **N10**-α, 19.9 and 174.3 J/g for **N11**-α, and 23.9 and 170.2 J/g for **N11**-γ.

Temperature Dependence of Infrared Spectra. (a) Amide Group Bands. Temperature dependence of infrared spectra in the frequency region 500−800 cm^{-1} is shown in Figure 2 a, b, and c for N10-α, N11-α, and N11-γ forms, respectively. Figure 3 a−c show the infrared spectra in the region 1300−1600 cm^{-1}. At room temperature **N11**-α and **N10**-α showed the infrared bands at 585 [amide VI (C═O out-of-plane mode)], 670 cm^{-1} [amide V (NH out-of-plane mode)], 1638 cm^{-1} [amide I (C═O stretching mode)], 1548 cm^{-1} [amide II (coupling of C−N stretching mode with N−H in-plane bending mode)], 3318 cm^{-1} [amide A (NH stretching mode)], and so on. All these bands are characteristic of the α form of nylons.[26−34] This is the reason these two model compounds were named the "α" form. These amide bands were found to shift the positions with increasing temperature in the region I, indicating a gradual weakening of hydrogen bonds between the neighboring amide groups. In the temperature region II, these bands decreased in intensity and the new bands appeared discontinuously at 630, 710, and 1570 cm^{-1} and so on.

Different from these two cases, the **N11**-γ form did not show discontinuous spectral change. The bands shifted apparently continuously toward the higher or lower frequency side (see Figures 2 and 3) and became broader in temperature region III. As will be mentioned later, the X-ray diffraction pattern was different between temperature regions I and III, and therefore the **N11**-γ form was found to exhibit a phase transition at the DSC peak of 70 °C. The high-temperature phase of the **N11**-γ form is designated as the γ_h form. Judging from the broad

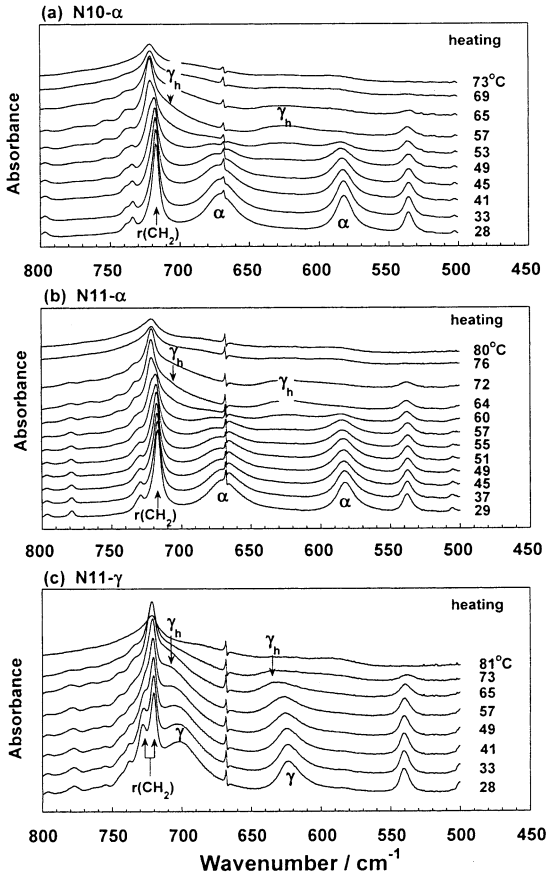

Figure 2. Temperature dependence of infrared spectra in the frequency region 500−800 cm^{-1}: (a) **N10**-α, (b) **N11**-α, and (c) **N11**-γ.

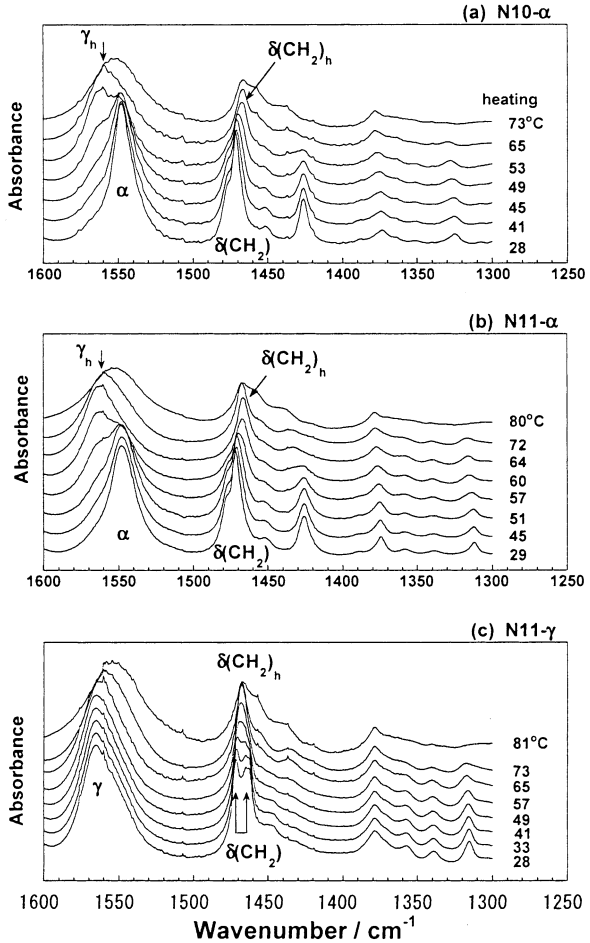

Figure 3. Temperature dependence of infrared spectra in the frequency region 1300−1600 cm^{-1}: (a) **N10**-α, (b) **N11**-α, and (c) **N11**-γ.

spectral pattern compared with that of the γ form at room temperature, the γ_h form may be structurally disordered more or less. This speculation is supported also by the X-ray diffraction data as will be mentioned later.

It should be noticed here that the infrared spectral pattern observed for **N11**-α and **N10**-α in the high-temperature region III is essentially the same with that observed for **N11**-γ form in the temperature region III. That is to say, the crystalline phase in the region III of **N11** and **N10** is considered to have essentially the same structure as that of the γ_h phase. Another point to be noted is a coexistence of amide bands of α and γ_h forms in the temperature region II of **N11** and **N10** (see Figures 2 and 3). The X-ray diffraction pattern measured in this temperature region was unique and could not be interpreted by a simple overlap of the patterns of these two crystal forms. It is considered that the intermediate phase takes some unique structure different from those of the α form (region I) and the γ_h form (region III), as will be discussed in a later section.

(b) Methylene Bands. *Subcell Structure.* As shown in Figure 2a,b, a relatively sharp band of the most in-phase methylene rocking mode was observed at 719 cm^{-1} in the spectra of **N10**-α and **N11**-α. This band is typical of the triclinic packing structure of *n*-alkane,[35,36] indicating that the methylene sequences are packed in a triclinic subcell. In the temperature regions II and III, a new band was detected around 723 cm^{-1} and the 719-cm^{-1} band decreased in intensity. The similar situation was observed also in the CH_2 scissoring mode region: the 1472-cm^{-1} band was replaced by the 1469-cm^{-1} band in the regions II and III. These newly observed bands were considered to come from the pseudohexagonal structure of methylene chain segments.[37−44] That is to say, a triclinic methylene packing structure in region I transformed to the pseudohexagonal form in regions II and III, as well-known in the case of *n*-alkane.[45,46] At the same time the bands corresponding to the disordered conformation composed of trans and gauche bonds were also detected in the transition temperature region: for example, the infrared spectral pattern in the region 1300−1470 cm^{-1} was similar to that observed for the pseudohexagonal phase of *n*-alkane.[37−44] In this way it may be reasonably said that the methylene segments are in a conformationally disordered state and are packed in a pseudohexagonal-type subcell in the high-temperature region.

In the case of **N11**-γ form, both the infrared bands of CH_2 rocking (720−730 cm^{-1}) and CH_2 scissoring (1460−1470 cm^{-1}) were doublets at room temperature. This observation was clearer in the infrared spectra taken at such a low temperature as liquid nitrogen temperature. These doublets are considered to be the so-called correlation splitting due to the neighboring methylene segments packed in the orthorhombic subcell.[47] As the temperature increased, the spectral profiles in these frequency regions started to change and approached gradually to the patterns characteristic of pseudohexagonal packing structure or the γ_h form. Different from the above-mentioned transition from the α to γ_h form, the transition from the γ to γ_h form occurred apparently continuously.

Progression Bands. As to the methylene vibrational modes, we cannot ignore a series of progression bands. For example, Figure 4 a, b, and c shows respectively the temperature dependence of infrared spectra measured for **N10**-α, **N11**-α, and **N11**-γ forms in the frequency region 750−1000 cm^{-1}. Most of the bands are the so-called progression bands, which are assignable to the CH_2 rocking and C−C stretching modes of

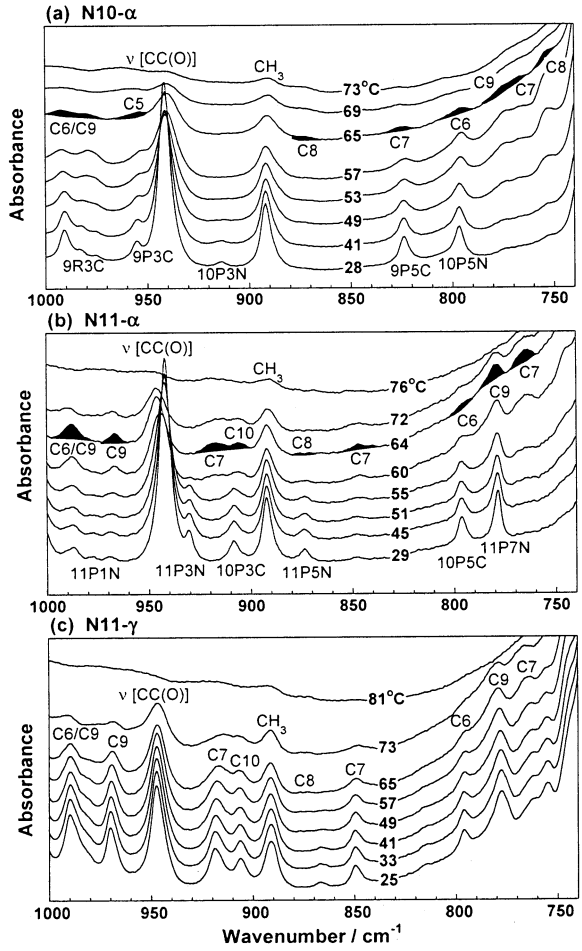

Figure 4. Temperature dependence of infrared progression bands in the frequency region 750−1000 cm^{-1}: (a) **N10**-α, (b) **N11**-α, and (c) **N11**-γ. Shaded bands appeared in the high-temperature region. The marks such as 10P5C indicate the vibrational modes assigned to each band. 10P5C, for example, indicates the rocking-twisting mode (P) of the methylene segment in the CO side (C) with $k = 5$, which is equivalent to the normal mode of the n-$C_{10}H_{22}$ chain. CH_3, methyl rocking mode; ν[CC(O)], C−C(O) stretching mode.

methylene sequence of finite chain length.[48−51] The progression bands observed for nylons and the model compounds, however, cannot be interpreted reasonably through the simple comparison with the infrared spectra of the corresponding *n*-alkane molecules.[52−59] The detailed explanation of this situation was made in the previous paper.[60] For example, a series of progression bands observed for a methylene segment sandwiched between the two amide groups, amide-$(CH_2)_m$-amide, cannot be compared with the progression bands of n-$C_{m+2}H_{2m+6}$[$CH_3(CH_2)_mCH_3$] but should be compared with those of n-C_mH_{2m+2}[$CH_3(CH_2)_{m-2}CH_3$]. That is to say, methylene units adjacent to the amide group need to be omitted, meaning that the vibrational coupling between the inner methylene segment and the outer methylene units is cut in the aliphatic nylon chain. Therefore, for the planar-zigzag methylene chain of **N11**-α form, the methylene sequences $CH_3(CH_2)_{10}$-NH and $CH_3(CH_2)_9CO$ are assumed to be equivalent to those of $CH_3(CH_2)_9CH_3$ (n-$C_{11}H_{24}$) and $CH_3(CH_2)_8CH_3$ (n-$C_{10}H_{22}$), respectively, from the viewpoint of vibrational modes. In this way, the progression bands of **N10**-α and **N11**-α forms shown in parts a and b of Figure 4, respectively, are assigned to the modes of *n*-alkanes indicated by small symbols. For example, 10P5C means that this band is equivalent to the progression band of the CH_2 rocking (P) mode with a phase angle between the neighboring methylene groups $\phi = k\pi/(m + 1) = 5\pi/(8+1) = 5\pi/9$ [a total number of effective methylene units (oscillators) $m = 8$ and $k = 5$]. A chain composed of eight methylene units is equivalent to n-$C_{10}H_{22}$ when two methyl groups are added as end groups. The "C" indicates that it is a mode of the methylene sequence of the carbonyl group side. Briefly speaking, 10P5C indicates the rocking (P) mode with $k = 5$ of the carbonyl side methylene sequence equivalent to n-$C_{10}H_{22}$. Similarly 10P5N indicates the mode of the methylene sequence in the NH side.

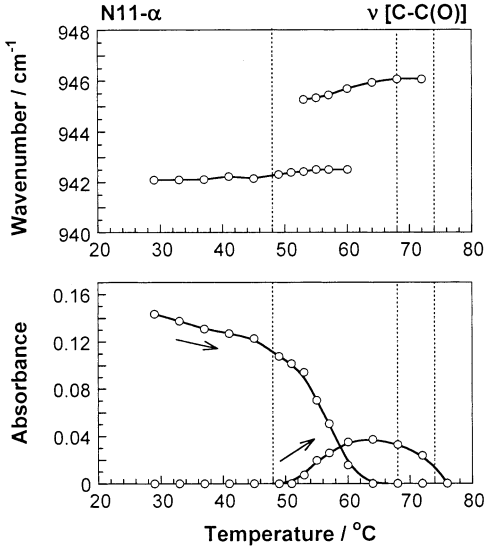

Figure 5. Temperature dependence of vibrational frequency and intensity estimated for the C−C(O) stretching band observed for the **N11**-α form.

When the **N10**-α and **N11**-α samples were heated, some of the progression bands disappeared above the transition point as seen in Figure 4a,b. (The temperature dependence of the infrared absorbance estimated for several progression bands will be shown in Figure 7 in a later section.) In the temperature region II the progression bands decreased in intensity remarkably and disappeared perfectly in the region III. In parallel, some new bands (shaded in Figure 4a,b) were observed. These bands were assigned to the vibrational modes of shorter *n*-alkane molecules by comparing the observed band positions with the vibrational frequencies reported for various *n*-alkane molecules with different chain lengths.[35,36,48−51] The assignments are given in Figure 4a,b. Most of the bands observed in the high-temperature regions were assigned to the modes of shorter alkane molecules: n-$C_{10}H_{22}$−n-C_6H_{14} for the γ_h phase of **N11** and n-C_9H_{20}−n-C_5H_{12} for the γ_h phase of **N10**. In other words, the fully trans-zigzag methylene sequence of the α form in the temperature region I changes to the conformationally disordered methylene segment consisting of shorter zigzag parts [$(CH_2)_8$−$(CH_2)_4$ for **N11** and $(CH_2)_7$−$(CH_2)_3$ for **N10**] plus some gauche bonds.

In the case of the **N11**-γ form, the spectral pattern of the progression bands did not change remarkably but was rather similar to that observed above the phase transition point. The progression bands at room temperature could not be assigned to the vibrational modes of all-trans methylene segments. As pointed out above, the infrared spectra in the temperature region III are common to **N10**-α, **N11**-α, and **N11**-γ forms, the pattern of the γ_h phase. Referring to the assignments made for the shaded bands in Figure 4b, the methylene segments of the γ form are speculated to contain such shorter trans parts as $(CH_2)_8$−$(CH_2)_4$. Existence of short trans segments means that the methylene segments are invaded by gauche bonds and are

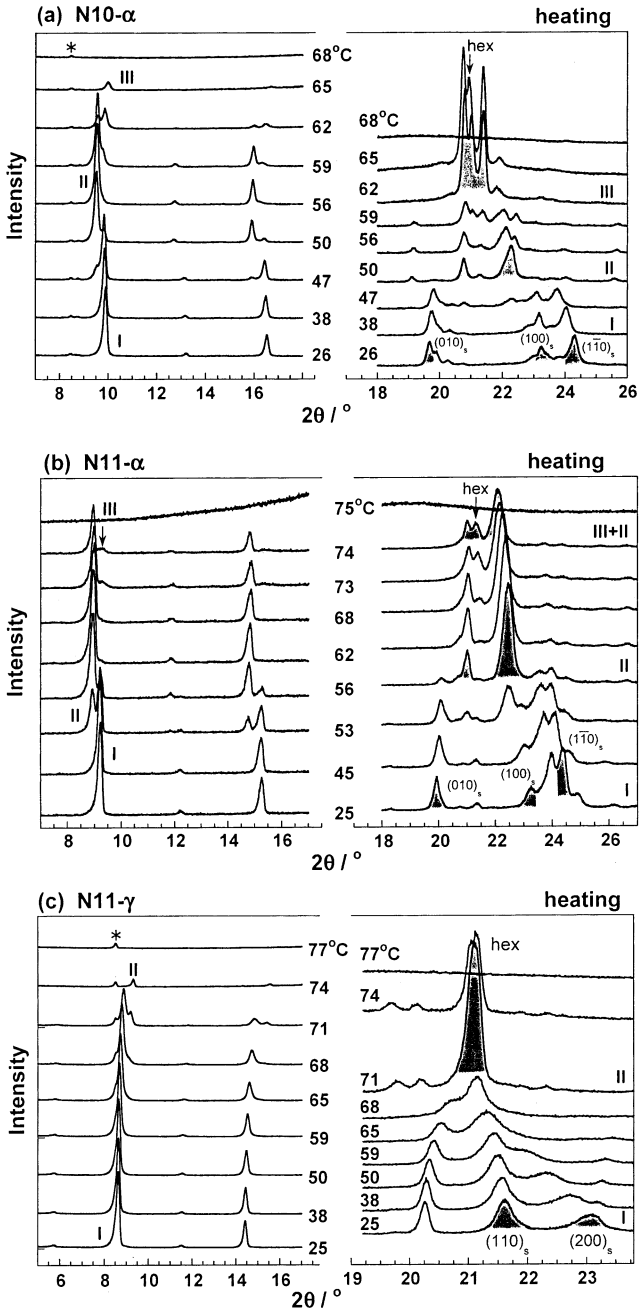

Figure 6. Temperature dependence of X-ray diffraction profile: (a) **N10**-α, (b) **N11**-α, and (c) **N11**-γ. The asterisks indicate the reflections coming from the sample cell.

conformationally disordered. As for a pair of bands generated by correlation spitting in the orthorhombic subcell, the relative intensity of 730-cm^{-1} band was appreciably lower than that of 720-cm^{-1} band even at room temperature, although it increased largely at low temperature. The relative intensity of the 730-cm^{-1} band is sensitive to the regularity of the packing structure of methylene chains.[61] Therefore the weak intensity of the 730-cm^{-1} band suggests that the relatively short trans methylene segments are packed together in the orthorhombic subcell in somewhat disordered manner. The disordered conformation was checked also by the observation of the spectral pattern in the region 1300−1450 cm^{-1}, as discussed in the previous section on the γ_h form.

(c) Other Bands. The other infrared bands useful for the discussion of structural change are C−C(O) and C−N stretching bands and methyl bands. In Figure 4b an intense C−C(O) stretching band was observed at 942 cm^{-1} for the **N11**-α form at room temperature. As plotted in Figure 5, the band decreased in intensity remarkably in temperature region II and a broad and weak band appeared at 945 cm^{-1}, which increased in intensity in regions II and III. A similar observation was made for the C−N stretching band at 1135 cm^{-1}. Amide V and VI bands were reported to be sensitive to the twisting angle around the CH_2–amide bonds (see Figures 2−4).[55] A remarkable intensity decrement observed for C−C(O) and C−N stretching bands suggests also an enhancement of such twisting motion.[62,63]

The band observed at 892 cm^{-1} is due to the rocking mode of the methyl group. The half width was found to increase in the transition from I to II (or III), indicating an enhancement of the rotational motion of methyl group in the high-temperature phase.[37−44] This phenomenon was commonly observed for **N11**-α, **N10**-α, and **N11**-γ samples.

From the temperature dependence of infrared spectra measured for **N11**-α, **N11**-γ, and **N10**-α forms, several characteristic structural changes may be extracted as listed below. The structural change is summarized in Table 1.

(1) On heating the **N11**-α (and **N10**-α) sample, the CH_2-$NHCOCH_2$ part showed a structural change from TTT to STS̄ in the transition from region I (α phase) to regions II and III (γ_h phase). But the STS̄ conformation in the high-temperature γ_h phase is more or less disordered. In the case of **N11**-γ form, the structural change occurs apparently continuously to the γ_h phase.

(2) The hydrogen bonds are kept in the transitions.

(3) The all-trans-zigzag methylene sequence of the α form changes to the disordered conformation in the high-temperature γ_h phase. The methylene segments in the γ_h phase are composed of the short trans-zigzag segments of 8−4 methylene units combined with gauche bonds (in the case of **N11**). The long trans segments in the α phase are packed in a triclinic subcell, while the conformationally disordered methylene segments of the γ_h phase are packed in a pseudohexagonal manner. In the case of the **N11**-γ form, the trans-zigzag methylene segments are not so long as that of the α form due to the invasion of gauche bonds, and these short trans segments are packed in the orthorhombic subcell in a somewhat disordered manner. In temperature region III, it transfers to the pseudohexagonal packing of the γ_h phase apparently continuously.

Temperature Dependence of X-ray Diffraction Pattern. (a) N10-α. Figure 6a shows the temperature dependence of the X-ray diffraction profile measured for the **N10**-α form. Since the X-ray structure analysis was not made for the single crystal, the indexing of the observed X-ray reflections was impossible. But, by tracing the temperature dependence of the reflections, we may extract the reflections representing the subcell structure of the methylene segments. For example, the main three peaks at 19.7°, 23.3°, and 24.3° detected at room temperature are considered to correspond respectively to the $(010)_s$, $(100)_s$, and $(1\bar{1}0)_s$ peaks of the triclinic structure, as well-known for the *n*-alkanes.[45,46] The parameters of the subcell were estimated as $a_s' = a_s \sin \beta_s' = 4.11$ Å, $b_s' = b_s \sin \alpha_s' = 4.85$ Å, and $\gamma_s' = 111.8°$, which corresponded relatively well to the triclinic cell parameters of *n*-alkanes: $a_s' = 4.07$ Å, $b_s' = 4.74$ Å and $\gamma_s' = 111.2°$.[45,46] The molecular chains are considered to form a stacked layer structure as judged from a series of reflections in the low scattering angle region. The long spacing of this layer stack or the interlayer spacing is about 26.7 Å. By taking into account the chain length of fully extended conformation of the α form, 29.6 Å, the interlayer spacing indicates a chain tilt by about 26° from the normal to the layer plane.

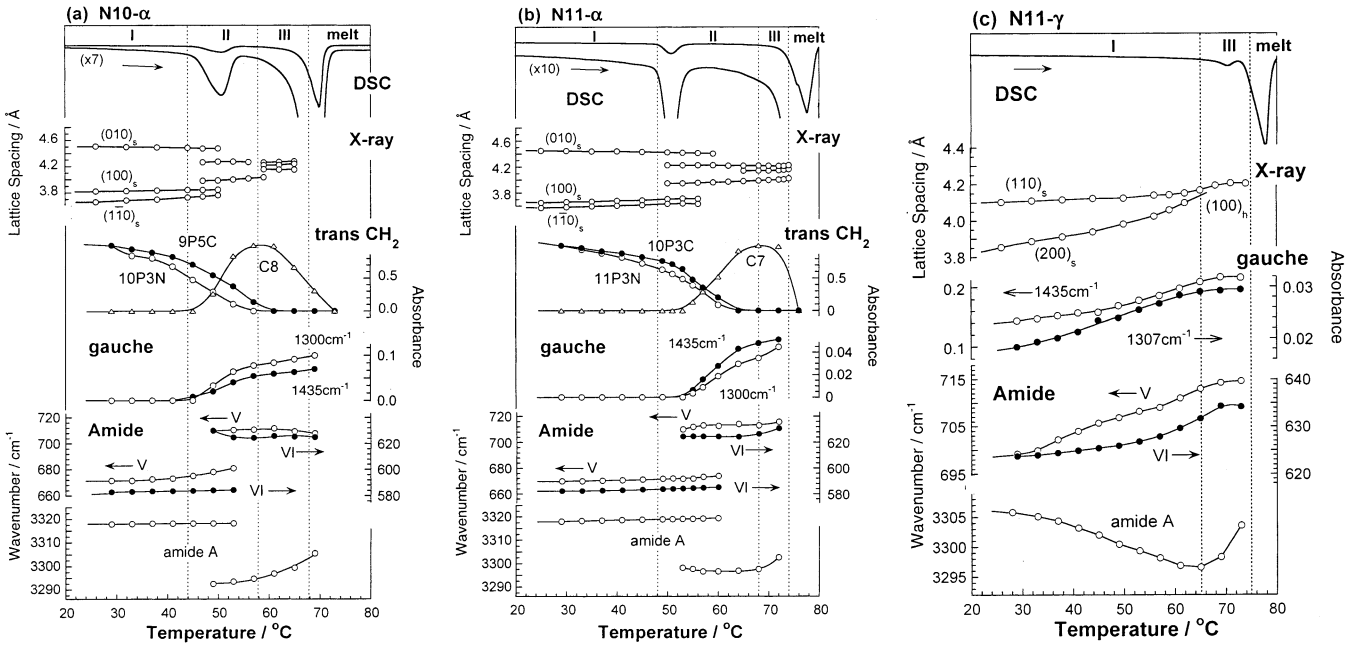

Figure 7. Comparison of DSC, X-ray diffraction, and infrared data collected in the heating process from the room temperature: (a) **N10**-α, (b) **N11**-α, and (c) **N11**-γ.

TABLE 1: Structural Changes Estimated from the Temperature-Dependent Infrared Spectral Data of N10-α, N11-α, and N11-γ Forms

⟨**N11**-α, **N10**-α⟩	region I	region II	region III
CH_2-amide-CH_2 methylene	TTT (α form)	TTT + $ST\bar{S}$	$ST\bar{S}$ (disordered) (γ_h form)
subcell	triclinic	triclinic + pseudohexagonal	pseudohexagonal
conformation	regular (all-trans)	I + III	disordered (short trans + gauche)
hydrogen bonds	strong	less strong	weak
⟨**N11**-γ⟩	region I		region III
CH_2-amide-CH_2 methylene	$ST\bar{S}$ (γ form)		$ST\bar{S}$ (disordered) (γ_h form)
subcell	less ordered orthorhombic		pseudohexagonal
conformation	short trans + gauche		disordered (short trans + gauche)
hydrogen bonds	strong		weak

The X-ray pattern was found to change at two stages in the transition-temperature regions. In temperature region II, the X-ray diffraction pattern was quite different from those observed in regions I and III. The temperature dependence of the lattice spacings of several reflections is shown in Figure 7a. In the DSC thermogram shown in Figure 1, the thermal energy change was difficult to detect in region II, but the X-ray diffraction indicated clearly an occurrence of some discontinuous structural change in the transition process from region I to II and from region II to III. The structure in region I is of the α form. The high-temperature γ_h phase in region III is of the pseudohexagonal packing consisting of conformationally disordered chains. The lattice parameter of the pseudohexagonal subcell was $a_s' = 8.4$ Å, corresponding to the value of $a_s = 8.3$ Å ($b_s = a_s/\sqrt{3}$) observed for the pseudohexagonal phase of *n*-alkanes.[45,46] In this way the X-ray diffraction data in the temperature regions I and III are reasonably interpreted and are consistent with the infrared data. But the X-ray diffraction pattern in the region II is unique. The detailed discussion about the structure in region II will be made in a later paragraph.

(b) N11-α. The temperature dependence of the X-ray diffraction pattern measured for the **N11**-α form is shown in Figure 6b. In Figure 7b the lattice spacings are plotted against temperature. The X-ray pattern at room temperature was similar to that of **N10**-α form: the cell parameters were estimated as $a_s' = 3.95$ Å, $b_s' = 4.82$ Å, and $\gamma_s' = 112.5°$. The diffraction pattern was quite different in regions I, II, and III, although the DSC thermogram did not show detectable heat change in region II. The interlayer spacing changed discontinuously from 29.0 Å in region I, to 29.9 Å in region II, and to 28.9 Å in region III.

(c) N11-γ. Figure 6c shows the temperature dependence of X-ray diffraction pattern of the **N11**-γ form. The two reflections located at 21.7° and 23.1° were assigned to the $(110)_s$ and $(200)_s$ peaks of the orthorhombic subcell structure with $a_s = 7.70$ Å and $b_s = 4.84$ Å, consistent with the corresponding cell parameters of *n*-alkanes and polyethylene (7.40 and 4.93 Å).[64] These two peaks changed their positions remarkably with increasing temperature and merged into a sharp reflection at 21.1° above 70 °C, as shown in Figure 7c, indicating the apparently continuous transition from the orthorhombic subcell (region I) to the pseudohexagonal subcell (region III). This change is consistent with the aforementioned infrared spectral change. The interlayer spacing was changed discontinuously from 30.6 Å in region I to 29.0 Å in III. Although the $(110)_s$ and $(200)_s$ reflections shifted continuously to one intense reflection as mentioned above, many new peaks appeared discontinuously in region III as seen in the scattering angle of 19−23° in Figure 6c. That is to say, the transition between regions I and III is essentially discontinuous as a whole crystal lattice, although the subcell structure of methylene segments changed apparently smoothly to the pseudohexagonal type.

Structural Change in Phase Transitions. (a) N10-α and N11-α Samples. Parts a and b of Figure 7 summarize respectively the main data collected for **N10**-α and **N11**-α samples through the measurements of X-ray diffraction and infrared spectra. These two samples show essentially the same transition behavior. In temperature region I the molecular chains take the trans-zigzag conformation in both the amide and methylene parts. The methylene chain segments are packed in a triclinic subcell and are bonded by intermolecular hydrogen bonds. In region III the methylene segments are conformationally disordered and the trans length becomes shorter because of the invasion of gauche bonds, as seen from the decrease in progression bands of long trans segments and the generation of the progression bands of shorter segments and gauche bands. The CH_2-amide-CH_2 part is twisted as seen from the generation of amide V and VI bands corresponding to the $ST\bar{S}$ conformation. These conformationally disordered chains are packed in a hexagonal mode. Although the strength is weaker, the intermolecular hydrogen bonds are kept alive even in this high-temperature region. In region II, both the molecular structural features in regions I and III are coexistent, although the chain packing structure is unique.

(b) N11-γ Sample. Figure 7c is the case of **N11**-γ sample in the heating process. In the transition from region I to III, the X-ray diffraction transfers from the pattern of the orthorhombic subcell to that of the pseudohexagonal subcell, as seen from the fusion of reflections $(110)_s$ and $(200)_s$ into the $(100)_h$ reflection where the subscript h means a hexagonal cell. The temperature dependence of the infrared band splittings in the CH_2 rocking and scissoring regions support this structural change (see Figures 2c and 3c). The structure in region III is essentially the same as that of **N11**-α. As discussed before, the γ form in region I is considered to be already disordered to some extent. As the temperature increases, the degree of disordering is increased and the structure approaches gradually to the structure in region III. But this apparently continuous transition is only for the chain conformation and subcell structure. As seen in the discontinuous change of the stacked layer structure, the whole crystal experiences a first-order-type phase transition.

(c) Possible Structure in Region II. Now let us consider the chain packing structure in the region II observed for **N10**-α and **N11**-α samples. The X-ray pattern of region II was different from those of regions I and III. But the infrared spectra were approximately an overlap of the patterns in the regions I (α) and III (γ_h). This can be said for both the amide bands and the methylene progression bands. By taking into consideration the structural features in regions I and III, we may have several possible structural models for region II, as illustrated in Figure 8. For convenience, the structures in regions I and III are now called simply the α and γ_h forms, respectively.

Figure 8a is a mixture of the stacking structures of the α and γ_h forms. Figure 8b is a stacking of layers consisting of only α or γ_h structures. In these two cases the X-ray diffraction pattern reflecting an inner-layer structure may be an overlap of the two patterns coming from the α and the γ_h structures, inconsistent with the observed data. Model c shows the other type of chain packing, in which one molecular chain is built up by combining the two types of conformation: a regular all-trans zigzag form (α form) on one side of the amide group and an irregular skewed form (γ_h form) on the other side. These chains are packed in a layer so that the regular and irregular parts are gathered separately on opposite sides of the amide groups. In model d these chains are packed in a random way. Model e is a random packing of the regular and irregular chains in one layer. At the present stage we cannot choose the best of these models.

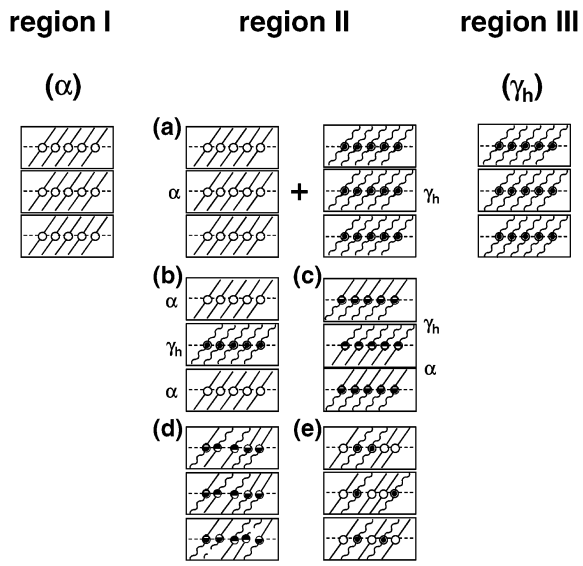

Figure 8. Illustration predicted for the structures **N11**-α and **N10**-α. The circle indicates the amide group and the straight and wavy lines indicate the regular and irregular conformations of methylene chains, respectively. Models (a)−(e) show possible candidates for the structure of phase II: (a) a mixture of the chain stacking structure of the α and γ forms; (b) a stacking of layers consisting of the α and γ forms; (c) a stacking of layers composed of molecular chains with regular and irregular methylene segments; (d) a random stacking of layers composed of molecular chains with regular and irregular methylene segments; (e) a random packing of the regular and irregular chains in one layer.

Conclusions

In the present paper we have described for the first time the phase transition behavior of **N10** and **N11**, which are the shortest model compounds of nylon 10/10 and 11/11, respectively. These two samples take the structure of the α form at room temperature. **N11** crystallizes also to the γ form. The infrared amide bands were found to change remarkably from TTT to $ST\bar{S}$ structure in the phase transition. At the same time the methylene chain changed conformation from the planar-zigzag all-trans form to the disordered form consisting of shorter zigzag chain segments combined with the gauche bonds. Based on the quantitative analysis of a series of progression bands, the length of zigzag chain part in region III was estimated to be $(CH_2)_4$−$(CH_2)_8$ for **N11** and $(CH_2)_3$−$(CH_2)_7$ for **N10**. The packing structure of methylene segments was of triclinic type in region I and of pseudohexagonal type in region III. During the transition the hydrogen bonds were kept alive, although the bonding strength became weaker. The infrared spectral pattern in region II was apparently an overlap of the patterns of regions I and III, but the X-ray diffraction pattern in region II was quite different from those of regions I and III, indicating an existence of a unique structure in region II. In this region, it was speculated that the structural features of the α and γ_h forms remained in one layer. The structural change illustrated in Figure 9 is the most plausible at present, which satisfies all the observed data of infrared spectra and X-ray diffraction consistently.

The crystal structure of γ form was considered more or less disordered even at room temperature. The trans-zigzag methylene segments were short and the gauche bonds were coexistent in the methylene chain. The trans methylene parts were packed in a disordered orthorhombic subcell, which transferred to the pseudohexagonal cell in the high-temperature region III. In the

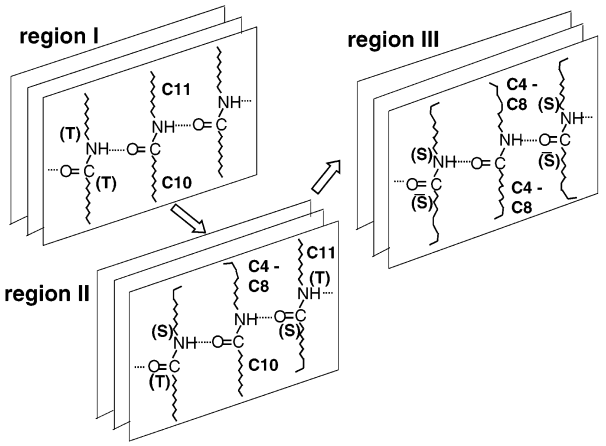

Figure 9. Illustration of the structures in the temperature regions I, II, and III speculated for **N11**-α and **N10**- α forms.

case of nylons the methylene sequence of the γ form takes a triclinic subcell structure,[27] while the γ form of **N11** takes the orthorhombic subcell structure. Combination of the STS̄ amide structure and orthorhombic packing of methylene segments is difficult in nylon crystals. **N11** was able to take an orthorhombic subcell structure because the chain ends were free.

In this way the model compounds **N10** and **N11** were found to show a large structure change in the transition regions, which is considered to correspond to the so-called Brill transition of nylons. As seen in Figure 7, conformational disordering occurs continuously but the X-ray diffraction pattern changes discretely in the transition region from I to II, for example. The transition from II to III is also in a similar situation. It is difficult now to uniquely assign these transitional features to the thermodynamic first- or second-order transition because of the too complicated structural changes. As discussed elsewhere, one of the characteristic points of the Brill transition is that the structure changes in a wide temperature region even when the sample is a low-molecular-weight compound. We need to investigate the transition behavior in more detail in order to clarify the essential features of the Brill transition. Anyway, however, the model compounds used here are too short in molecular length compared with the parent nylons. We will report the transition behavior of the compounds with longer repeating units and compare them with the behavior described here in a near future.

References and Notes

(1) Brill, R. J. *J. Prakt. Chem.* **1942**, *161*, 49.
(2) Itoh, T. *Jpn. J. Appl. Phys.* **1976**, *15*, 2295.
(3) Newman, B. A.; Sham, T. P.; Pae, K. D. *J. Appl. Phys.* **1977**, *48*, 4092.
(4) Starkweather, H. W., Jr.; Jones, G. A. *J. Polym. Sci., Polym. Phys Ed.* **1981**, *19*, 467.
(5) Kim, K. G.; Newman, B. A.; Scheinbeim, J. I. *J. Polym. Sci., Polym. Phys. Ed.* **1985**, *23*, 2477.
(6) Hirschinger, J.; Miura, H.; Gardner K. H.; English A. D. *Macromolecules* **1990**, *23*, 2153.
(7) Murthy, N. S.; Curran, S. A.; Aharoni, S. M.; Minor H. *Macromolecules* **1991**, *24*, 3215.
(8) Radusch, H. J.; Stolp, M.; Androsch, R. *Polymer* **1994**, *35*, 3568.
(9) Hill, M. J.; Atkins, D. T. *Macromolecules* **1995**, *28*, 2642.
(10) Jones, N. A.; Atkins, E. D. T.; Hill, M. J.; Cooper, S. J.; Franco, L. *Polymer* **1997**, *38*, 2689.
(11) Jones, N. A.; Cooper, S. J.; Atkins, E. D. T.; Hill, M. J.; Franco, L. *J. Polym. Sci., B: Polym. Phys. Ed.* **1997**, *35*, 675.
(12) Cooper, S. J.; Atkins, E. D. T.; Hill, M. J. *Macromolecules* **1998**, *31*, 8947.
(13) Franco, L.; Cooper, S. J.; Atkins, E. D. T.; Hill, M. J.; Jones, N. A. *J. Polym. Sci., B: Polym. Phys. Ed.* **1998**, *36*, 1153.
(14) Murthy, N. S.; Wang, Z.; Hisao, B. S. *Macromolecules* **1999**, *32*, 5594.
(15) Jones, N. A.; Atkins, E. D. T.; Hill, M. J. *J. Polym. Sci., B: Polym. Phys. Ed.* **2000**, *38*, 1209.
(16) Ramesh, C.; Gowd E. B. *Macromolecules* **2001**, *34*, 3308.
(17) Yang, X.; Tan, S.; Li, G.; Zhou, E. *Macromolecules* **2001**, *34*, 5936.
(18) Biangardi, H. J. *J. Macromol. Sci., Phys.* **1990**, *B29*, 139.
(19) Vasanthan, N.; Murthy, N. S.; Bray, R. G. *Macromolecules* **1998**, *31*, 8433.
(20) Tereshko, V.; Vidal, X.; Goodman, M.; Subirana, J. A. *Macromolecules* **1995**, *28*, 837.
(21) Cooper, S. J.; Atkins, E. D. T.; Hill, *J. Polym. Sci., B: Polym. Phys. Ed.* **1998**, *36*, 2849.
(22) Cooper, S. J.; Atkins, E. D. T.; Hill, M. J. *Macromolecules* **1998**, *31*, 5032.
(23) Escudero, E.; Subirana, J. A.; Solans, X. *Acta Crystallogr.* **1999**, *C55*, 644.
(24) Escudero, E.; Subirana, J. A. *Macromolecules* **2001**, *34*, 837.
(25) Bunn, C. W.; Garnar, E. V. *Proc. R. Soc.* **1947**, *A189*, 39.
(26) Miyake, A. *J. Polym. Sci.* **1960**, *44*, 223.
(27) Arimoto, H. *J. Polym. Sci. A* **1964**, *2*, 2283.
(28) Matsubara, I.; Itoh, Y.; Shinomiya, M. *Polym. Lett.* **1966**, *4*, 47.
(29) Komatsu, T.; Makino, D.; Kobayashi, M.; Tadokoro, H. *Rep. Prog. Polym. Phys. Jpn* **1970**, *13*, 1051.
(30) Jakes, J.; Krimm, S. *Spectrochim. Acta* **1971**, *27A*, 35.
(31) Skrovanek, D. J.; Painter, P. C.; Colemen, M. M. *Macromolecules* **1986**, *19*, 9, 699.
(32) Maddam, W. F.; Royaud, I. A. M. *Spectrochim. Acta* **1991**, *47A*, 1327.
(33) Schmidt, P.; Hendra, P. J. *Spectrochim.* **1994**, *50A*, 1999.
(34) Yu, H. H. *Mater. Chem. Phys.* **1998**, *56*, 289.
(35) Snyder, R. G. *J. Mol. Spectrosc.* **1960**, *4*, 411.
(36) Snyder, R. G. *J. Mol. Spectrosc.* **1961**, *7*, 116.
(37) Strobl, G. R.; Ewen, B.; Fischer, E. W.; Piesczek, W. *J. Chem. Phys.* **1974**, *61*, 5257.
(38) Ewen, B.; Fischer, E. W.; Piesczek, W.; Strobl, G. R. *J. Chem. Phys.* **1974**, *61*, 5265.
(39) Ewen, B.; Strobl, G. R.; Richter, D. *J. Chem. Soc., Faraday Dsicuss.* **1980**, *69*, 19.
(40) Snyder, R. G.; Maroncelli, M.; Qi, S. P.; Strauss, H. L. *Science* (Washinton, D.C.) **1981**, *214*, 188.
(41) Maroncelli, M.; Qi, S. P.; Strauss, H. L.; Snyder, R. G. *J. Am. Chem. Soc.* **1982**, *104*, 6237.
(42) Maroncelli, M.; Strauss, H. L.; Snyder, R. G. *J. Chem. Phys.* **1985**, *82*, 2811.
(43) Hagemann, H.; Strauss, H. L.; Snyder, R. G. *Macromolecules* **1987**, *20*, 2810.
(44) Kim, Y.; Strauss, H. L.; Snyder, R. G. *J. Phys. Chem.* **1989**, *93*, 7520.
(45) King, H. E.; Sirota, E. B., Jr.; Singer, D. M. *J. Phys. D; Appl. Phys.* **1993**, *26*, B133.
(46) Sirota, E. B.; King, H. E.; Singer, D. M., Jr.; Shao, H. H. *J. Chem. Phys.* **1995**, *98*, 5809.
(47) Krimm, S.; Liang, C. Y.; Sutherland, G. B. B. M. *J. Chem. Phys.* **1956**, *25*, 549.
(48) Nielsen, J. R.; Holland, R. F. *J. Mol. Spectrosc.* **1960**, *4*, 448.
(49) Nielsen, J. R.; Holland, R. F. *J. Mol. Spectrosc.* **1961**, *6*, 394.
(50) Snyder, R. G.; Schachtschneider, J. H. *Spctrochim. Acta* **1963**, *19*, 85.
(51) Schachtschneider, J. H.; Snyder, R. G. *Spctrochim. Acta* **1963**, *19*, 117.
(52) Schneider, B.; Schmidt, P.; Wichterle, O. *Collect. Czech. Chem. Commun.* **1962**, *27*, 1749.
(53) Jakes, J.; Schmidt, P.; Schneider B. *Collect. Czech. Chem. Commun.* **1965**, *30*, 996.
(54) Jakes, J. *J. Polym. Sci. C* **1967**, *16*, 305.
(55) Jakes, J.; Krimm, S. *Spectrochimica Acta* **1971**, *27A*, 19.
(56) Raman, R.; Deopura, L. B.; Varma, D. S. *Indian J. Textile Res.* **1977**, *2*, 56.
(57) Biangardi, H. J. *J. Macromol. Sci., Phys.* **1990**, *B29*, 139.
(58) Vasanthan, N.; Murthy, N. S.; Bray, R. G. *Macromolecules* **1998**, *31*, 8433.
(59) Cooper, S. J.; Coogan, M.; Everall, N.; Priestnall, I. *Polymer* **2001**, *42*, 10 119.
(60) Yoshioka, Y.; Tashiro, K. *J. Polym. Sci., B: Polym. Phys. Ed.* **2003**, *41*, 1294.
(61) Tashiro, K.; Sasaki, S.; Kobayashi, M. *Macromolecules* **1996**, *29*, 7460.
(62) Hirschinger, J.; Miura, H.; Gardner K. H.; English A. D. *Macromolecules* **1990**, *23*, 2153.
(63) Wendoloski, J. J.; Gardner, K. H.; Hirschinger, J.; Miura, H.; English, A. D. *Science* (Washinton, D.C.) **1990**, *247*, 431.
(64) Bunn, C. W. *Trans. Faraday Soc.* **1939**, *35*, 482.